IOP Publishing Biomed. Mater. 18 (2023) 015006 https://doi.org/10.1088/1748-605X/ac9f90

Biomedical Materials

PAPER

Enzymatically crosslinked hydrogel based on tyramine modified gelatin and sialylated chitosan

Peng Ding[1,2,*], Qianqian Wei[1], Ning Tian[1], Xiaoyue Ding[1], Ling Wang[1], Bin Wang[1], Oseweuba Valentine Okoro[3], Amin Shavandi[3,*] and Lei Nie[1,3,*]

[1] School of Life Science, Xinyang Normal University, Xinyang 464000, People's Republic of China
[2] Tea Plant Biology Key Laboratory of Henan Province, Xinyang 464000, People's Republic of China
[3] Université libre de Bruxelles (ULB), École polytechnique de Bruxelles, 3BIO-BioMatter, Avenue F.D. Roosevelt, 50 - CP 165/61, 1050 Brussels, Belgium
[*] Authors to whom any correspondence should be addressed.

E-mail: dingzhiyu120@163.com, amin.shavandi@ulb.be, nieleifu@yahoo.com and nielei@xynu.edu.cn

Keywords: chitosan, sialic acid, tyramine, gelatin, hydrogel

RECEIVED
17 September 2022

REVISED
19 October 2022

ACCEPTED FOR PUBLICATION
2 November 2022

PUBLISHED
15 November 2022

Abstract

The enzymatically crosslinked hydrogel could replicate the cellular microenvironment for biomedical applications. In the present study, to improve the cytocompatibility of chitosan (CS), sialic acid (SA) was introduced to CS to synthesize sialylated CS (CS-SA), and the tyramine (TA) was grafted to gelatin (G) to obtain TA modified gelatin (G-TA). The successful synthesis of CS-SA and G-TA was confirmed using ^{1}H NMR and UV–Vis absorption spectra. The interpenetrating polymer networks G-TA/CS-SA (GC) hydrogel was then fabricated via blending G-TA and CS-SA solutions and crosslinked using horseradish peroxidase. The storage modulus (G′) of the fabricated GC hydrogels with different ratios of G-TA/CS-SA greatly varied during the formation and strain of hydrogels. With the increase of CS-SA concentration from 0% to 2%, the storage modulus of GC hydrogels was also observed to decrease from 1500 Pa to 101 Pa; the water uptake capacity of GC hydrogels increased from 1000% to 4500%. Additionally, the cell counting kit-8 and fluorescent images demonstrated the excellent cytocompatibility of GC hydrogels after culturing with NIH 3T3 cells. The obtained results indicated that the fabricated GC hydrogels might have potential in biomedical fields, such as wound dressing.

1. Introduction

Hydrogels crosslinked with hydrophilic polymer networks are widely considered promising materials for tissue engineering and regenerative medicine [1–4]. The hydrated structure of hydrogels facilitates oxygen and nutrient transfer to create a peripheral environment similar to the native extracellular matrix and thus promotes cell proliferation, differentiation, and gene expression [5–8]. Natural polymers such as fibrin, alginate, collagen, hyaluronic acid, gelatin and chitosan have been investigated as functional biomaterials for hydrogel production, with gelatin considered particularly promising. This is because gelatin constitutes the main extracellular component of connective tissues, including cartilage, bone and skin [5, 7, 9–17] and is rich in arginine-glycine-aspartic (RGD) peptide sequence. The abundance of the RGD peptide sequence enabled gelatin's integration with hyaluronic acid, poly(ethylene glycol), alginate and silk fibroin to improve their bioactivity for skin [18–27], cartilage [13, 14, 28–33] and nerve tissue engineering applications [34, 35]. Chitosan is another natural polymer that has been used for biomedical materials due to its biodegradability, anti-infection activity, biocompatibility and hemostatic activity, although its applicability is limited by its poor solubility in aqueous solution [36]. Chitosan possesses many reactive functional hydroxyl and amino/acetamido groups that facilitate diverse chemical modifications to produce various chitosan-based hydrogels for various biological applications [7, 23, 25, 37]. Song *et al* [38], prepared the hydrogel adhesive by integrating polyvinyl alcohol and catechol groups modified chitosan, and durable and repeatable adhesiveness was reinforced because of the limited auto-oxidation of catechol groups of the 3-(3,4-dihydroxyphenyl) propionic acid

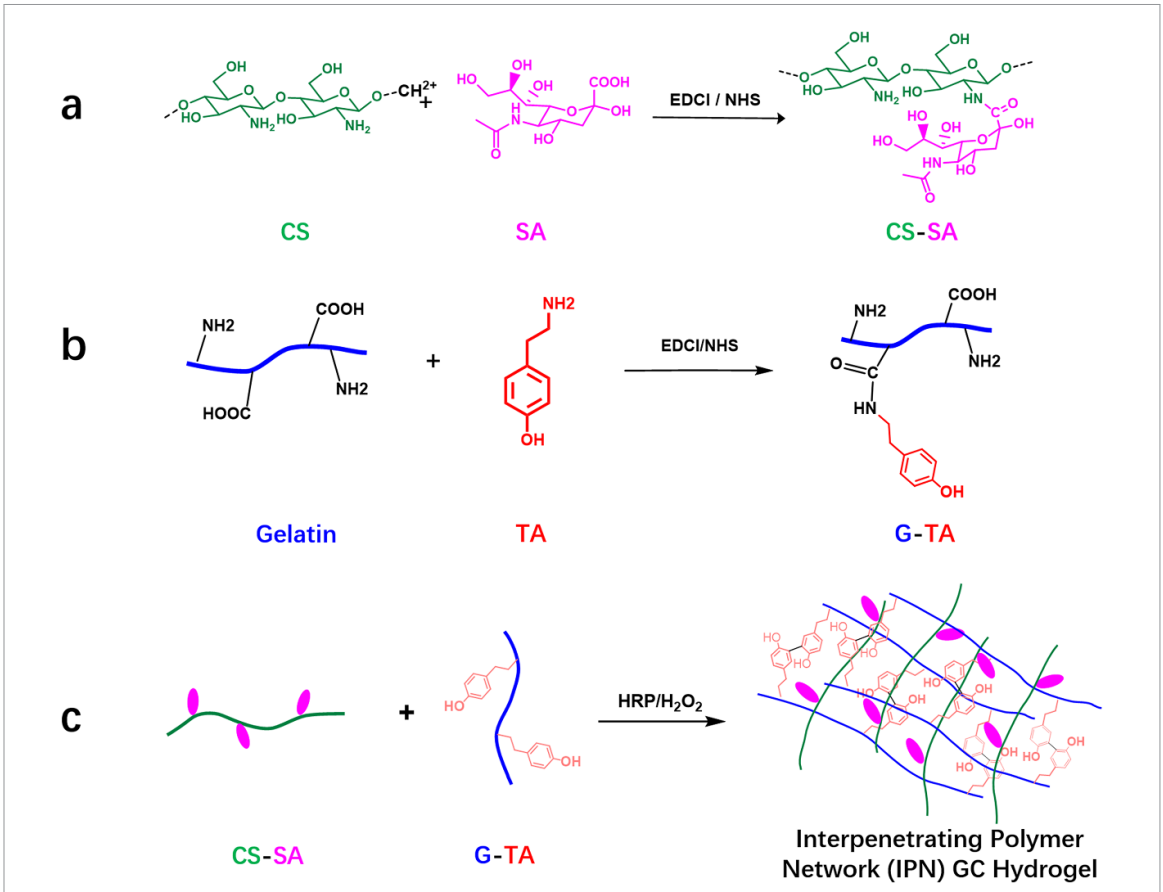

Figure 1. Schematic representation of IPN GC hydrogel by an enzyme-catalysed oxidation reaction. (a) Synthesis of sialic acid grafted chitosan (CS-SA). (b) Carbodiimide coupling of tyramine (TA) to carboxylic acid residues on gelatin. (c) HRP-mediated covalent crosslinking of G-TA and the formation of IPN GC hydrogels.

modified chitosan. The designed hydrogel displayed potential in tissue adhesion and wound healing applications.

It is acknowledged that stereospecific saccharide-saccharide interactions at the cell surface perform essential roles in various cellular processes, such as cell adhesion, signalling and recognition [39–44]. For instance, oligosaccharide Lewis (X)-Lewis (X) interaction induces cell adhesion in embryonic development [45], and dissociated sponge cells from two different species can reaggregate through surface proteoglycans in a Ca^{2+}-rich environment by sorting out according to their species of origin [46]. Moreover, in previous articles, mono- or di-saccharide groups were creatively introduced into a polymeric interface material to enhance the affinity to glycopeptides based on saccharide-saccharide interactions [47–49]. These examples inspire an investigation into introducing a saccharide group such as sialic acid (SA) to a hydrogel surface to potentially enhance interaction between cells and materials for enhanced cell biocompatibility of materials.

In addition, the interpenetrating polymer networks (IPNs) hydrogels using the combination of two or more topologically interlocking polymer chains could readily achieve favourable mechanical properties and recapitulate complex cell-matrix interactions [50]. Among the various methods of hydrogel preparation, enzyme-mediated cross-linking of chemically formed hydrogels has attained much attention due to its high substrate specificity and efficacy [51]. Importantly, unlike other chemical cross-linking reactions that involve photo-initiators [52] and organic solvents [53, 54], there is no risk of unwanted side effects or toxicity in the enzymatic hydrogelation systems. Horseradish peroxidase (HRP) is one of the enzymes that has been used to catalyze the cross-linking of phenol or aniline derivatives in the presence of H_2O_2 [55, 56]. Compared with other enzymatic hydrogelation mechanisms (tyrosinase, transglutaminase, phosphatases, etc), HRP-crosslinked hydrogels have become more popular for use in different biomedical applications because of their excellent, adjustable mechanical properties [57, 58]. This study had therefore sought to investigate the modification of chitosan with sialic acid (N-acetylneuraminic acid) (CS-SA) and the functionalization of gelatin with tyramine (G-TA) to produce IPN hydrogels. The *in situ* forming IPN G-TA/CS-SA (GC) hydrogels will be developed using the enzymatic oxidative reaction of HRP and H_2O_2 [59], and the physicochemical properties and cytocompatibility of the prepared IPN GC hydrogels subsequently be evaluated (figure 1).

2. Experimental section

2.1. Materials

Chitosan (CS, SKU: 448 855, degree of deacetylation: 75–85%, medium molecular weight, viscosity: 200–800 cP), SA, 3-(4-hydroxyphenyl) propionic acid (HPA), N-hydroxysuccinimide (NHS), morpholinoethanesulfonic acid (MES), 1-ethy-3-(3-dimethylaminopropyl carbodiimide) hydrochloride (EDC·HCl, EDCI) and HRP (300 IU mg^{-1}) were purchased from Aladdin Co., Ltd (Shanghai, China). Gelatin type A (SKU: 924 504-IEA, powder) was purchased from Merck Co., Ltd Dimethylformamide (DMF) and hydrogen peroxide (H_2O_2) were bought from Sinopharm Chemical Reagent Co., Ltd All chemicals and solvents purchased were used as received without further purification.

2.2. Synthesis of sialylated chitosan (CS-SA)

Briefly, chitosan (1.2 g) was fully dissolved in 200 ml of 1 wt% acetic acid aqueous solution, followed by pH adjustment to 6 using 5 M NaOH. SA (2.0 g), EDCI (3.7 g), and NHS (1.7 g), were dissolved in a 0.1 M MES buffer solution (50 ml) and stirred for 30 min and subsequently added to the chitosan solution [60]. The solution was stirred (500 rpm) at 22 °C for 12 h, with the resulting sialylated chitosan product subsequently dialyzed against Millipore water using a 7000 Da molecular weight cutoff dialysis membrane for three days, followed by lyophilization.

2.3. Synthesis of gelatin conjugates (G-TA)

Gelatin (2.5 g) was dissolved in 100 ml of Millipore water at 60 °C and stirred for 1 h to facilitate complete dissolution. NHS (15 mg) and EDCI (25 mg) were added to HPA (20 mmol) and dissolved in 100 ml of a co-solvent of DMF and water (volume ratio of 2:3). Then, the activated HPA solution was transferred to the gelatin solution, and the mixture reacted at 40 °C for 12 h. Finally, the resulting solution was dialyzed against Millipore water for three days and subsequently lyophilized to facilitate product recovery [2].

2.4. Preparation of enzymatically crosslinked IPN GC hydrogels

After a couple of pre-experiments to prepare GC hydrogels, the following method was used to fabricate GC hydrogels. The prepared G-TA was dissolved in phosphate buffer (pH at 7.4), and then the CS-SA was added to the G-TA solution to obtain G-TA/CS-SA composite solution. About 10 µl of H_2O_2 solution (167 mM) and 10 µl of HRP solution (1000 U ml^{-1}) were added to each tube, and 1 ml of G-TA/CS-SA composite solution was added, respectively. Then, the IPN GC hydrogel was formed by gentle stirring of the two solutions. The nomenclature of the as-prepared GC hydrogels is expressed as follows: X–C–Y, where X represents the concentration of G-TA and Y represents the concentration of CS-SA. In this work, samples 5C0, 5C1, 5C2, 8C0, 8C1, and 8C2 were prepared.

2.5. ^{1}H nuclear magnetic resonance (NMR) analysis

A proton ^{1}H NMR spectrometer was used to investigate the chemical composition of CS, SA, CS-SA, gelatin, and G-TA. The polymers were dissolved in deuterium oxide (D_2O), and ^{1}H NMR measurements were performed on a 600 MHz NMR spectrometer (ECZ600R/S3, JEOL RESONANCE Inc., Japan) equipped with a 14.09 T superconducting magnet and a 5.0 mm 600 MHz broadband Z-gradient high-resolution ROYAL probe.

2.6. UV-Vis analysis

The UV-Vis spectra of gelatin and G-TA were tested using Ultraviolet-visible spectroscopy (UV–Vis, PerkinElmer Lambda 950, USA). The samples were dissolved in distilled water at 0.1% (w/w), and the introduced phenolic hydroxyl (Ph) groups in G-TA were confirmed by detecting the absorbance at 275 nm.

2.7. Rheology analysis

Rheological measurement of the prepared GC hydrogels was performed using a rheometer (TA, DHR, USA) equipped with a 20 mm stainless steel upper cone and temperature-controlled Peltier bottom plate (DISCOVERY HR-2, TA, USA), at 37 °C [61]. Briefly, a 420 µl aliquot of pre-hydrogel solutions with 2.5 U ml^{-1} HRP was loaded to the Peltier, and the cone was lowered to a specified gap. Low-viscosity oil was placed around the outside edge of the cone to prevent water evaporation. Meanwhile, 4.2 µl of 0.5 vol.% H_2O_2 was injected into the gap to initiate the gelation. A dynamic time sweep was conducted at 1 Hz with 1% applied strain for 4000 s to determine gelation kinetics and storage moduli. Following gelation, dynamic frequency sweeps (0.1–100 rad s^{-1} at 1% strain) and strain sweeps (0.1%–500% or to failure, at 1 Hz) were performed to analyze the elastic behaviour of the resulting hydrogels.

2.8. Water uptake (WU) analysis

The WU of the prepared GC hydrogels was measured using a gravimetric method at 22 °C. Briefly, the as-prepared cylindrical hydrogel samples were fully immersed in phosphate-buffered saline (PBS) buffer at 22 °C [4]. The swollen samples were weighed at specific time intervals until they reached swelling equilibrium. Then, the hydrogels were freeze-dried until a constant weight was obtained. The WU of the hydrogels in PBS buffer was then calculated as follows;

$$\mathrm{WU} = \frac{W_s - W_d}{W_d} \quad (1)$$

where W_s is the mass in g of the swollen hydrogel sample and W_d is the dry mass in g of the hydrogel sample.

2.9. SEM analysis

The morphology of the cross-section of GC hydrogels was characterized by SEM. The lyophilized as-prepared GC hydrogels were immersed in liquid nitrogen for rapid freezing. The samples were then cut off using a sharp blade. The cut cross-sections were then sprayed with platinum for 40 s, and the morphology was subsequently observed using a cold field emission scanning electron microscopy (SEM, Hitachi, S-4800) with an accelerating voltage of 10 kV imposed. At least five SEM images at different magnifications were randomly obtained for each sample, then the pore size was calculated using ImageJ Software.

2.10. Cell counting kit-8 (CCK-8) analysis

The cytocompatibility of the GC hydrogels was conducted by evaluating the viability of NIH 3T3 cells cultured with the GC hydrogels. CCK-8 was used to investigate the viability of NIH 3T3 cells after seeding on GC hydrogels and culturing for different days. The optical density (O.D) value at 450 nm was measured to indicate the presence of metabolically active NIH 3T3 cells, and cells cultured without hydrogels as a control group [9]. The NIH 3TS cells (CRL-1658^{TM}, American Type Culture Collection(ATCC)) were grown in Dulbecco's modified Eagle's medium with 10% fetal bovine serum, 100 U ml^{-1} penicillin, and 100 μg ml^{-1} streptomycin under a humidified atmosphere of 5% CO_2 and 95% air at 37 °C, according to ATCC instruction. Cells at passage 5 for the next experiments. The prepared GC hydrogels were soaked in 75% of alcohol overnight and replaced by PBS on the ultra-clean working table. All hydrogels were added to a 48-well plate (Corning), and 1 ml of NIH 3TS cells solution was added to each well (1×10^4 cells ml^{-1}), and incubated at 37 °C in a 5% CO_2 atmosphere, using the culture medium as a control. After incubating for one day, two days, and three days, the samples were treated with CCK-8 kit solution (10 μl), and then incubated for 2 h at 37 °C. Finally, the reaction solutions were transferred to a 96-well plate. The O.D at 450 nm for each well was tested using a microplate reader (Tecan GENios, Tecan Austria GmbH, Salzburg, Austria).

2.11. Fluorescent microscopy analysis

The phalloidin-FTTC and 4′6-diamidino-2-phenylindole (DAPI) were used to stain the cells seeded in the prepared GC hydrogels. The procedure was described in our previous report [12]. Briefly, the hydrogels were cultured with NIH 3TS cells for three days, the hydrogels were washed using PBS and fixed with 2% glutaraldehyde for 10 min. Then the hydrogels were washed with PBS and treated using 0.1% of Triton X-100, then phalloidin-FITC and DAPI were subsequently used. Finally, the treated hydrogels were washed using PBS again, and the fluorescent microscopy images were obtained using a confocal laser scanning microscope (Leica TCS SP5 II, Germany).

2.12. Statistical analysis

All experiments were conducted in triplicate, and the data were expressed as means with standard deviation. The statistical package for the social sciences (SPSS) software (IBM SPSS Statistics, Version 26) was used for the analysis. Analysis of variance (ANOVA) statistical analyses and Tukey's test were applied to investigate specific differences between the control group and tested group for CCK-8 results. Statistical significance was defined at a p-value of < 0.05 and < 0.01 for 95% and 99% confidence, respectively.

3. Results and discussion

3.1. Synthesis and characterization of CS-SA and G-TA

Chitosan is an insoluble nature polymer in neutral aqueous solutions [62]. In this work, the chitosan was modified by reacting SA with primary amino groups of chitosan through EDCI/NHS activation to improve its water solubility (figure 1(a)). The successful synthesis of CS-SA was evaluated using the ^{1}H NMR spectra analysis (figure 2(a)). As shown in the spectrum of CS-SA, chemical shifts at 2.99, 3.48–3.74 ppm were assigned to the hydrogen protons of [H1] and [H2]–[H5], respectively. As for the ^{1}H NMR spectrum of SA, peaks at 1.77, 1.88, 3.38, 3.44, 3.58 and 3.66 ppm were assigned to the hydrogen protons of [H6], [H9], [H7], [H11], [H10], [H8], respectively. However, the ^{1}H NMR spectrum signal of the raw chitosan did not initially have the above peaks, with the peaks becoming visible when in the ^{1}H NMR spectrum signal of the CS-SA conjugate, confirming the successful graft of SA to chitosan. The successful introduction of phenol groups was confirmed using UV–Vis spectrum analysis with the UV–Vis spectra of G and G-TA displayed in figure 2(b). The absorbance detection at a peak 275 nm in the UV–Vis spectrum confirmed the successful synthesis of G-TA. Such a result could also be confirmed using ^{1}H NMR analysis (figure 2(c)). The ^{1}H NMR spectrum of G-TA clearly showed that the integration value corresponding to phenol groups (6.5–7.2 ppm) was much higher than that of gelatin, indicating the conjugation of TA to gelatin backbones.

3.2. Rheological analysis and WU of GC hydrogels

The GC hydrogel could be obtained by mixing G-TA/CS-SA/H_2O_2 and G-TA/CS-SA/HRP solutions with gentle shaking, and the formation of GC hydrogel could be evaluated by a tube inversion method (figure 3(a)) [63, 64]. The prepared GC hydrogels

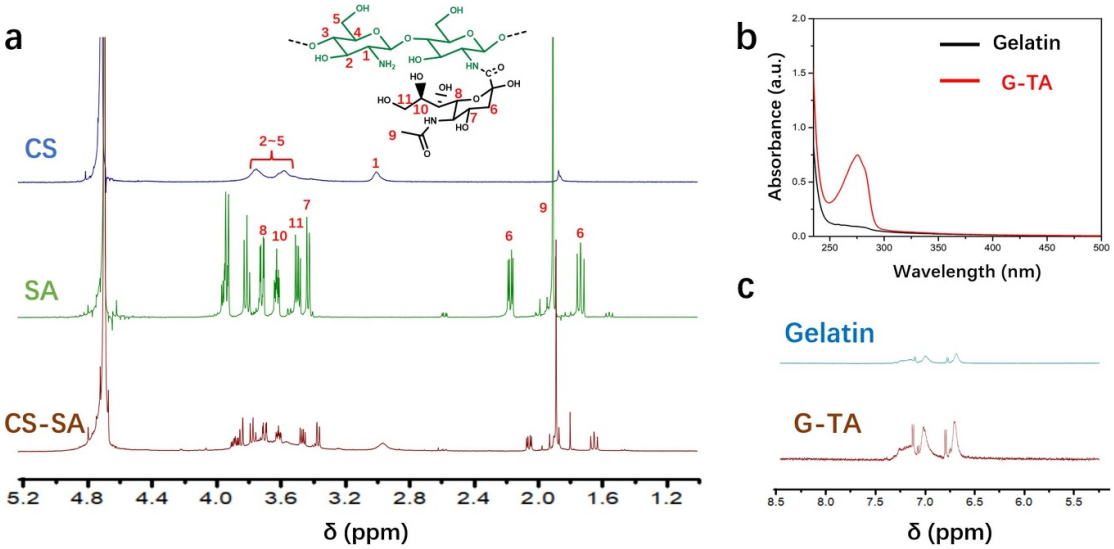

Figure 2. (a) ^{1}H NMR spectra (D_2O) of CS, SA and CS-SA, (b) UV–Vis spectra of gelatin and G-TA, (c) ^{1}H NMR spectra (D_2O) of gelatin and G-TA.

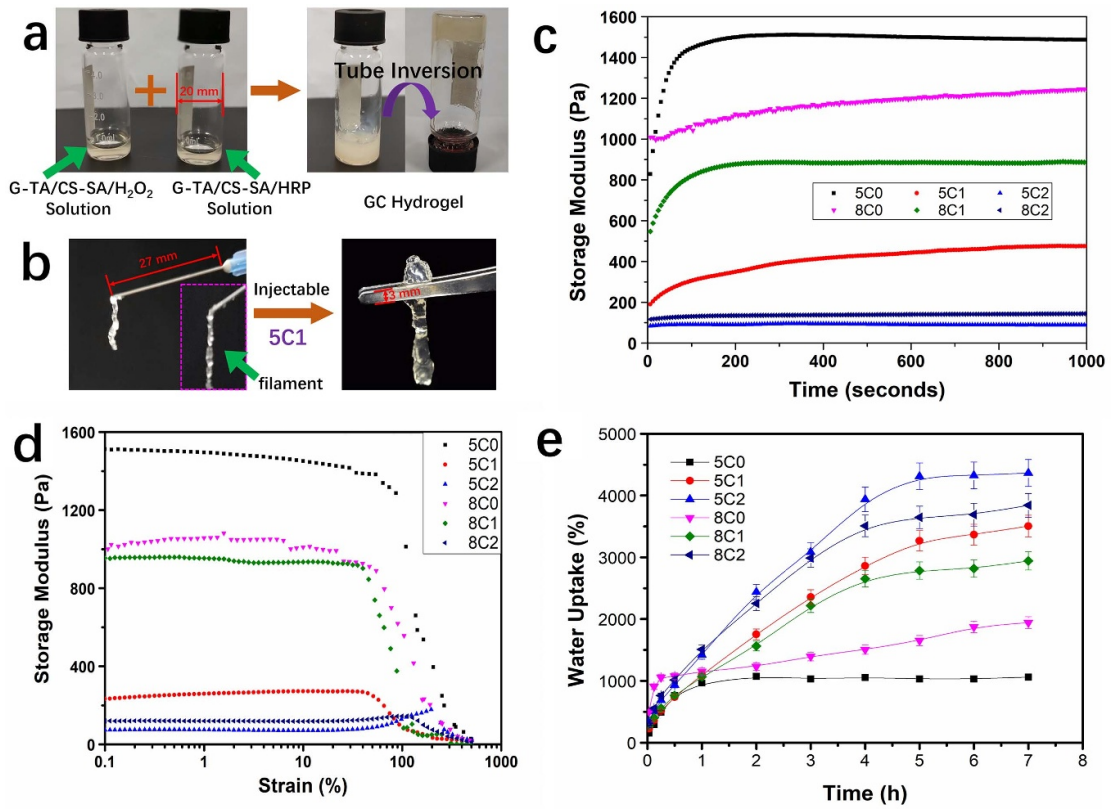

Figure 3. (a) The HRP/H_2O_2 mediated *in situ* formed GC hydrogel could be prepared by compositing G-TA/CS-SA/H_2O_2 and G-TA/CS-SA/HRP solutions, the hydrogel formation was identified using the tube inversion method. (b) The GC hydrogel (5C1) could be injected using a syringe, and the filament was formed. Rheological properties of GC hydrogels, (c) representative time sweeps, (d) strain sweeps. (e) Water uptake capacity of GC hydrogels.

could be injected using a syringe, and the filament was obtained, confirming the injectability of GC hydrogels (figure 3(b)) [65]. Next, the kinetics of gelation and mechanical properties of the prepared GC hydrogels were assessed using oscillatory rheology experiments (figures 3(c) and (d)). The GC hydrogels of varying CS-SA and G-TA concentrations containing HRP and H_2O_2 were *in situ* formed in a cone and plate geometry, maintained at 37 °C. Figure 3(c) displayed that all the samples with mixing the polymer solutions increased the storage modulus (G′) due to enzymatically crosslinked reactions of G-TA, until a plateau value was attained, indicating a plateau value at the end of the crosslinking process.

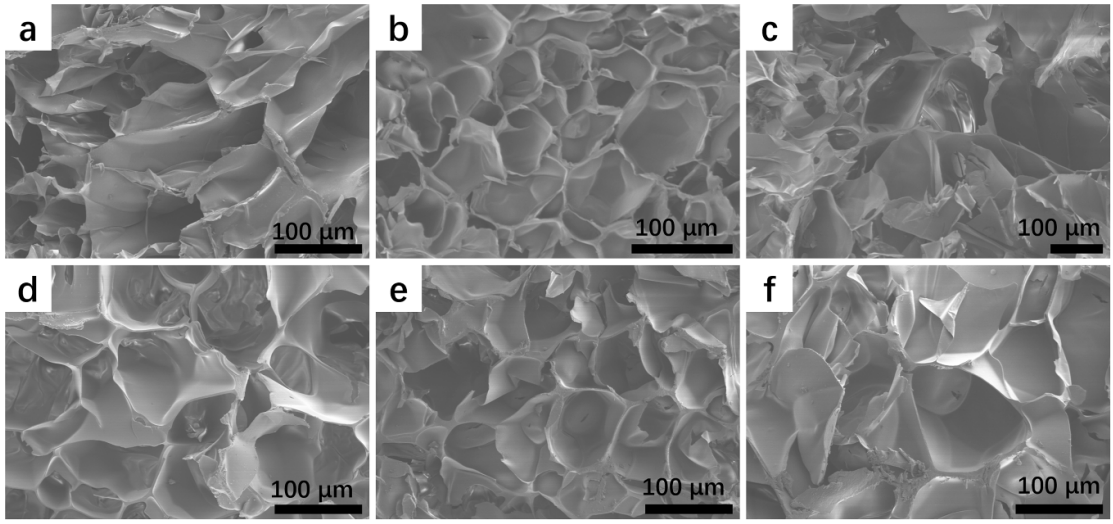

Figure 4. SEM images of the prepared GC hydrogels after freezed-dried, (a) 5C0, (b) 5C1, (c) 5C2, (d) 8C0, (e) 8C1, and (f) 8C2.

It was observed that a higher G-TA concentration resulted in a higher storage modulus, while the storage modulus decreased as the CS-SA content increased. In addition, the linear viscoelastic region was also conducted by the strain amplitude sweep at a range of 0.1%–500% at 1 Hz (figure 3(d)), with the storage modulus of all the prepared GC hydrogels shown to remain constant in a wide range of strain. This observation indicated that the GC hydrogels had a highly stable structure under a relatively high degree of deformations. Notably, however, the storage modulus was observed to decrease with an increase in CS-SA content. For the prepared GC hydrogels, the simultaneous IPN would be formed after mixing G-TA/CS-SA/H_2O_2 and G-TA/CS-SA/HRP solutions, CS-SA polymer chains spread in both solutions, and then the G-TA polymer network formed with the enzymatic oxidative reaction of HRP and H_2O_2 (figure 1(c)) [50, 59, 66].

The WU capacity is an essential feature of the hydrogels because it relates to other properties, including their mechanical properties and pore size, which further influences nutrient transport, drug delivery and tissue exudate adsorption through hydrogels [67]. Figure 3(e) shows that the WU capacity of GC hydrogels increased from 1000% to 4500% as the CS-SA concentration increased from 0% to 2%. This is because of the hydration of the hydrophilic group SA group, which was grafted to the CS backbone. Therefore, the hydrophilicity of the as-prepared hydrogels was higher than the previous reports [68, 69]. It was also noticed that the sample 5C2 hydrogel with the highest CS-SA concentration displayed the highest WU capacity, which increased to 4300% after 7 h, compared to other samples. The WU capacity of GC hydrogels was also influenced by the G-TA content, which due to that, the enzymatically crosslink degree increased with the increase of G-TA concentration.

3.3. Microstructure of GC hydrogels

The microstructure of the cross-section of the as-prepared GC hydrogels (figure 4) showed a 3D, relatively homogeneous, and interconnected pore structure, which indicated good structural stability and uniform physical structure for all prepared GC hydrogels. In addition, the pore size of GC hydrogels was calculated using ImageJ software on 5 random SEM images from each sample. There was no great differences for all samples 5C0 (62.8 ± 7.1 μm), 5C1 (53.4 ± 5.6 μm), 5C2 (61.6 ± 8.3 μm), 8C0 (62.7 ± 9.2 μm), 8C1 (56.1 ± 6.9 μm), and 8C2 (59.1 ± 7.9 μm). However, the prepared gelatin/chitosan hydrogels crosslinked by HRP displayed a much more uniform pore size distribution, compared to the previous gelatin/chitosan hydrogels crosslinked via thiol-Michael addition reaction [52]. The porous interconnected structure provides enough space for cell growth, attachment, proliferation, and extracellular matrix secretion [14, 24, 69].

3.4. *In vitro* cytocompatibility evaluation

The cytocompatibility of the GC hydrogels was conducted by CCK-8 analysis after seeding NIH 3T3 cells on GC hydrogels and culturing for different days, as shown in figure 5. The viability of NIH 3T3 cells cultured on the hydrogels increased from day 1 to day 3, indicating a good cytocompatibility of the prepared GC hydrogels. On day 1, the cell viability on GC hydrogels was lower than that of the control group. However, the cell growth in GC hydrogels was higher on day 2, proving that proliferation of the cells in GC hydrogels was faster than that of the control group, which might be due to the 3D

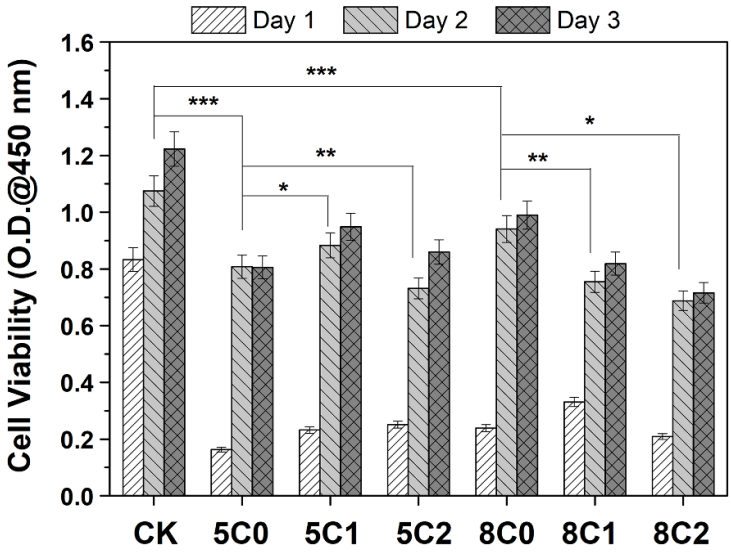

Figure 5. Cytocompatibility of the prepared GC hydrogels was evaluated by CCK-8 assay by culturing with NIH 3T3 cells for different days. $^{*}p < 0.05$, $^{**}p < 0.01$, and $^{***}p < 0.001$.

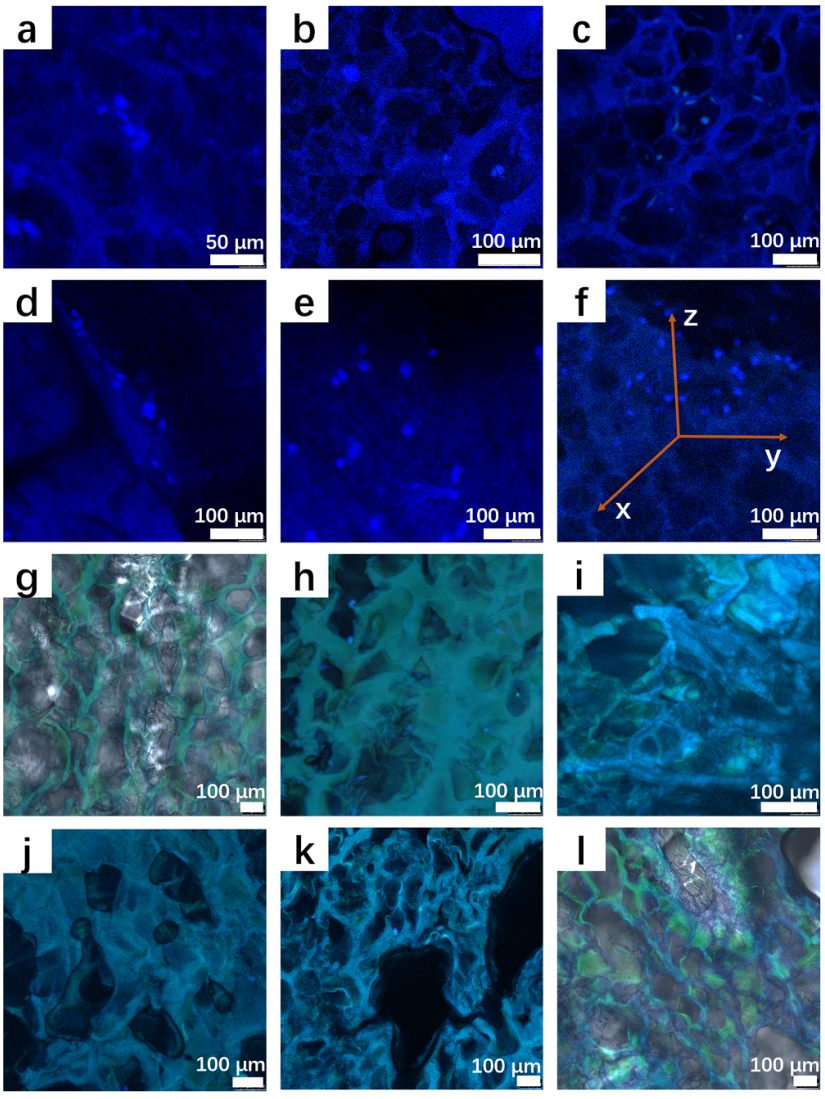

Figure 6. Representative fluorescent microscopy images of GC hydrogels cultured with NIH 3T3 cells for three days. The samples were stained using DAPI (a)–(f) and phalloidin-FITC/DAPI (g)–(l), respectively. (a) and (g) 5C0, (b) and (h) 5C1, (c) and (i) 5C2, (d) and (j) 8C0, (e) and (k) 8C1, and (f) and (l) 8C2.

micro-environment supported by GC hydrogels continuing to support the proliferation of cells. Enhancing the interaction between cells and the extracellular environment is of great importance to engineering functional biomaterial interfaces able to instruct cells with specific commands. On day 1, the cell viability seeded on GC hydrogels without CS-SA was lower than GC hydrogels with CS-SA. Here, it was worth mentioning that SA was introduced to the chitosan to enhance the interactions between cells and biomaterial interfaces based on carbohydrate-carbohydrate interactions suggested as mediators of cell adhesion and aggregation [42, 47, 49].

On day 3, sample 8C0 displayed the highest O.D value compared to other samples. The hydrogel 8C0 with the highest G-TA concentration possessed the highest crosslinking degree, providing a suitable framework and 3D micro-environment for cell growth. In addition, the NIH 3T3 cells seeded on GC hydrogels on day 3 were evaluated using fluorescent microscopy images (figure 6). Interestingly, the framework of the prepared GC hydrogels was stained due to the presence of polysaccharides in the hydrogels [7]. Thus, DAPI and phalloidin-FITC/DAPI were both used respectively to investigate the growth of cells and the microstructure of hydrogels. The porous interconnected structure for all GC hydrogels was observed after the NIH 3T3 cells were seeded and cultured for three days, consistent with SEM images of GC hydrogels in a dry state. For samples stained using DAPI alone, some cells could be observed (figures 6(a)–(f)). The cells seeded hydrogels were stained using phalloidin-FITC/DAPI, however, it was difficult to identify the cells (figures 6(g)–(l)). With the proliferation of cells on GC hydrogels over days, the cells grew and diffused into the hydrogels; thus, not many cells were observed on the surface of hydrogels. CCK-8 and fluorescent microscopy images confirmed the cytocompatibility of the prepared GC hydrogels.

4. Conclusion

The enzyme-mediated cross-linked hydrogels have displayed potentials in biomedical applications due to their high substrate specificity and efficacy. In this paper, we have devised an IPN GC hydrogel through the HRP-mediated crosslinking. A series of GC hydrogels based on CS-SA and G-TA with formulated compositions were prepared at physiological temperature. The GC hydrogels with interconnected structures could provide a suitable 3D microenvironment for cell adhesion and proliferation, confirmed by CCK-8 analysis and fluorescent microscopy images. The results in this paper suggest that these as-prepared enzymatically crosslinked IPN GC hydrogels have great potential as promising biomaterials for biomedical applications.

Data availability statement

The data that support the findings of this study are available upon reasonable request from the authors.

Acknowledgments

The authors acknowledge support from the Nanhu Scholars Program for Young Scholars of XYNU. Lei Nie acknowledges the support from YY. The authors acknowledge the help from Prof Lingling Wang, Professor Qiuju Zhou, Miss Zihe Jin, Dr Zongwen Zhang, and Dr Dongli Xu, in the Analysis & Testing Center of XYNU.

Conflict of interest

The authors declare no competing financial interest.

CRediT authorship contribution statement

Peng Ding: Conceptualization, Methodology, Software, Formal analysis, Writing—original draft, Data curation, Writing—review & editing. **Qianqian Wei:** Methodology, Software. **Ning Tian:** Data curation. **Xiaoyue Ding:** Data curation. **Ling Wang:** Data curation. **Bin Wang:** Data curation. **Oseweuba Valentine Okoro:** Writing—review & editing. **Amin Shavandi:** Conceptualization, Methodology, Writing—review & editing. **Lei Nie:** Conceptualization, Methodology, Software, Formal analysis, Writing—original draft, Writing—review & editing, Supervision.

ORCID iD

Lei Nie https://orcid.org/0000-0002-6175-5883

References

[1] Van Vlierberghe S, Dubruel P and Schacht E 2011 Biopolymer-based hydrogels as scaffolds for tissue engineering applications: a review *Biomacromolecules* **12** 1387–408
[2] Hasturk O, Jordan K E, Choi J and Kaplan D L 2020 Enzymatically crosslinked silk and silk-gelatin hydrogels with tunable gelation kinetics, mechanical properties and bioactivity for cell culture and encapsulation *Biomaterials* **232** 119720
[3] Wang L, Wu Y, Hu T, Ma P X and Guo B 2019 Aligned conductive core-shell biomimetic scaffolds based on nanofiber yarns/hydrogel for enhanced 3D neurite outgrowth alignment and elongation *Acta Biomater.* **96** 175–87
[4] Asadpour S, Kargozar S, Moradi L, Ai A, Nosrati H and Ai J 2020 Natural biomacromolecule based composite scaffolds from silk fibroin, gelatin and chitosan toward tissue engineering applications *Int. J. Biol. Macromol.* **154** 1285–94
[5] Lei Z, Zhu W, Zhang X, Wang X and Wu P 2021 Bio-inspired ionic skin for theranostics *Adv. Funct. Mater.* **31** 2008020
[6] Antoni D, Burckel H, Josset E and Noel G 2015 Three-dimensional cell culture: a breakthrough *in vivo Int. J. Mol. Sci.* **16** 5517–27

[7] Nie L, Deng Y, Li P, Hou R, Shavandi A and Yang S 2020 Hydroxyethyl chitosan-reinforced polyvinyl alcohol/biphasic calcium phosphate hydrogels for bone regeneration *Acs Omega* **5** 10948–57

[8] Jalalvandi E and Shavandi A 2019 Shear thinning/self-healing hydrogel based on natural polymers with secondary photocrosslinking for biomedical applications *J. Mech. Behav. Biomed. Mater.* **90** 191–201

[9] Nie L *et al* 2019 Development of chitosan/gelatin hydrogels incorporation of biphasic calcium phosphate nanoparticles for bone tissue engineering *J. Biomater. Sci. Polym. Ed.* **30** 1636–57

[10] Nie L, Chen D, Yang Q, Zou P, Feng S, Hu H and Suo J 2013 Hydroxyapatite/poly-l-lactide nanocomposites coating improves the adherence and proliferation of human bone mesenchymal stem cells on porous biphasic calcium phosphate scaffolds *Mater. Lett.* **92** 25–28

[11] Chen D, Zhang C X, Huo H J, Ji C C, Sun M and Nie L 2018 Injectable temperature-sensitive hydrogel with VEGF loaded microspheres for vascularization and bone regeneration of femoral head necrosis *Mater. Lett.* **229** 138–41

[12] Nie L *et al* 2019 Preparation and characterization of dithiol-modified graphene oxide nanosheets reinforced alginate nanocomposite as bone scaffold *SN Appl. Sci.* **1** 545

[13] Wang X, Tang S, Chai S, Wang P, Qin J, Pei W, Bian H, Jiang Q and Huang C 2021 Preparing printable bacterial cellulose based gelatin gel to promote *in vivo* bone regeneration *Carbohydrate Polym.* **270** 118342

[14] Xu J, Feng Q, Lin S, Yuan W, Li R, Li J, Wei K, Chen X, Zhang K and Yang Y 2019 Injectable stem cell-laden supramolecular hydrogels enhance *in situ* osteochondral regeneration via the sustained co-delivery of hydrophilic and hydrophobic chondrogenic molecules *Biomaterials* **210** 51–61

[15] Deng Y, Shavandi A, Okoro O V and Nie L 2021 Alginate modification via click chemistry for biomedical applications *Carbohydrate Polym.* **270** 118360

[16] Gu Y, Hu Y, Huang C, Lai C, Ling Z and Yong Q 2022 Co-production of amino acid-rich xylooligosaccharide and single-cell protein from paper mulberry by autohydrolysis and fermentation technologies *Biotechnol. Biofuels Bioprod.* **15** 1–10

[17] Huang C, Peng Z, Li J, Li X, Jiang X and Dong Y 2022 Unlocking the role of lignin for preparing the lignin-based wood adhesive: a review *Ind. Crops Prod.* **187** 115388

[18] Zheng K, Tong Y, Zhang S, He R, Xiao L, Iqbal Z, Zhang Y, Gao J, Zhang L and Jiang L 2021 Flexible bicolorimetric polyacrylamide/chitosan hydrogels for smart real-time monitoring and promotion of wound healing *Adv. Funct. Mater.* **31** 2102599

[19] Zhou L, Pi W, Cheng S, Gu Z, Zhang K, Min T, Zhang W, Du H, Zhang P and Wen Y 2021 Multifunctional DNA hydrogels with hydrocolloid-cotton structure for regeneration of diabetic infectious wounds *Adv. Funct. Mater.* **31** 2106167

[20] Fan Y, Lüchow M, Zhang Y, Lin J, Fortuin L, Mohanty S, Brauner A and Malkoch M 2021 Nanogel encapsulated hydrogels as advanced wound dressings for the controlled delivery of antibiotics *Adv. Funct. Mater.* **31** 2006453

[21] Yin X, Hao Y, Lu Y, Zhang D, Zhao Y, Mei L, Sui K, Zhou Q and Hu J 2021 Bio-multifunctional hydrogel patches for repairing full-thickness abdominal wall defects *Adv. Funct. Mater.* **31** 2105614

[22] Tu Z, Chen M, Wang M, Shao Z, Jiang X, Wang K, Yao Z, Yang S, Zhang X and Gao W 2021 Engineering bioactive M2 macrophage-polarized anti-inflammatory, antioxidant, and antibacterial scaffolds for rapid angiogenesis and diabetic wound repair *Adv. Funct. Mater.* **31** 2100924

[23] Guo S, Yao M, Zhang D, He Y, Chang R, Ren Y and Guan F 2022 One-step synthesis of multifunctional chitosan hydrogel for full-thickness wound closure and healing *Adv. Healthcare Mater.* **11** 2101808

[24] Yang X, Li P, Tang W, Du S, Yu M, Lu H, Tan H and Xing X 2021 A facile injectable carbon dot/oxidative polysaccharide hydrogel with potent self-healing and high antibacterial activity *Carbohydrate Polym.* **251** 117040

[25] Gu B, Jiang Q, Luo B, Liu C, Ren J, Wang X and Wang X 2021 A sandwich-like chitosan-based antibacterial nanocomposite film with reduced graphene oxide immobilized silver nanoparticles *Carbohydrate Polym.* **260** 117835

[26] Peng X, Xu X, Deng Y, Xie X, Xu L, Xu X, Yuan W, Yang B, Yang X and Xia X 2021 Ultrafast self-gelling and wet adhesive powder for acute hemostasis and wound healing *Adv. Funct. Mater.* **31** 2102583

[27] Choi C, Kim S and Cha C 2021 Dual-functional alginate crosslinker: independent control of crosslinking density and cell adhesive properties of hydrogels via separate conjugation pathways *Carbohydrate Polym.* **252** 117128

[28] Seo B-B, Kwon Y, Kim J, Hong K H, Kim S-E, Song H-R, Kim Y-M and Song S-C 2022 Injectable polymeric nanoparticle hydrogel system for long-term anti-inflammatory effect to treat osteoarthritis *Bioact. Mater.* **7** 14–25

[29] Zhu M, Zhong W, Cao W, Zhang Q and Wu G 2022 Chondroinductive/chondroconductive peptides and their-functionalized biomaterials for cartilage tissue engineering *Bioact. Mater.* **9** 221–38

[30] Kazemi-Aghdam F, Jahed V, Dehghan-Niri M, Ganji F and Vasheghani-Farahani E 2021 Injectable chitosan hydrogel embedding modified halloysite nanotubes for bone tissue engineering *Carbohydrate Polym.* **269** 118311

[31] Yue K, Li X, Schrobback K, Sheikhi A, Annabi N, Leijten J, Zhang W, Zhang Y S, Hutmacher D W and Klein T J 2017 Structural analysis of photocrosslinkable methacryloyl-modified protein derivatives *Biomaterials* **139** 163–71

[32] Zhang Y, Dou X, Zhang L, Wang H, Zhang T, Bai R, Sun Q, Wang X, Yu T and Wu D 2022 Facile fabrication of a biocompatible composite gel with sustained release of aspirin for bone regeneration *Bioact. Mater.* **11** 130–9

[33] Huang W, Cheng S, Wang X, Zhang Y, Chen L and Zhang L 2021 Noncompressible hemostasis and bone regeneration induced by an absorbable bioadhesive self-healing hydrogel *Adv. Funct. Mater.* **31** 2009189

[34] Yang S, Zhu J, Lu C, Chai Y, Cao Z, Lu J, Zhang Z, Zhao H, Huang Y-Y and Yao S 2022 Aligned fibrin/functionalized self-assembling peptide interpenetrating nanofiber hydrogel presenting multi-cues promotes peripheral nerve functional recovery *Bioact. mater.* **8** 529–44

[35] Boni R, Ali A, Shavandi A and Clarkson A N 2018 Current and novel polymeric biomaterials for neural tissue engineering *J. Biomed. Sci.* **25** 90

[36] Nosrati H, Khodaei M, Alizadeh Z and Banitalebi-Dehkordi M 2021 Cationic, anionic and neutral polysaccharides for skin tissue engineering and wound healing applications *Int. J. Biol. Macromol.* **192** 298–322

[37] Jalalvandi E and Shavandi A 2018 *In situ*-forming and pH-responsive hydrogel based on chitosan for vaginal delivery of therapeutic agents *J. Mater. Sci. Mater. Med.* **29** 158

[38] Song F, Zhang J, Lu J, Cheng Y, Tao Y, Shao C and Wang H 2021 A mussel-inspired flexible chitosan-based bio-hydrogel as a tailored medical adhesive *Int. J. Biol. Macromol.* **189** 183–93

[39] Jung H Y, Le Thi P, HwangBo K-H, Bae J W and Park K D 2021 Tunable and high tissue adhesive properties of injectable chitosan based hydrogels through polymer architecture modulation *Carbohydrate Polym.* **261** 117810

[40] Cummings R D and Pierce J M 2014 The challenge and promise of glycomics *Chem. Biol.* **21** 1–15

[41] Handa K and Hakomori S-I 2012 Carbohydrate to carbohydrate interaction in development process and cancer progression *Glycoconj. J.* **29** 627–37

[42] Lorenz B R, Alvarez de Cienfuegos L, Oelkers M, Kriemen E, Brand C, Stephan M, Sunnick E, Yüksel D, Kalsani V and Kumar K 2012 Model system for cell adhesion mediated by weak carbohydrate–carbohydrate interactions *J. Am. Chem. Soc.* **134** 3326–9
[43] Hakomori S 2004 Carbohydrate-to-carbohydrate interaction, through glycosynapse, as a basis of cell recognition and membrane organization *Glycoconj. J.* **21** 125–37
[44] Ding L, Cheng W, Wang X, Ding S and Ju H 2008 Carbohydrate monolayer strategy for electrochemical assay of cell surface carbohydrate *J. Am. Chem. Soc.* **130** 7224–5
[45] Kojima N, Fenderson B A, Stroud M R, Goldberg R I, Habermann R, Toyokuni T and Hakomori S-I 1994 Further studies on cell adhesion based on Lex-Lex interaction, with new approaches: embryoglycan aggregation of F9 teratocarcinoma cells, and adhesion of various tumour cells based on Lex expression *Glycoconj. J.* **11** 238–48
[46] Fernàndez-Busquets X and Burger M M 2003 Circular proteoglycans from sponges: first members of the spongican family *Cell. Mol. Life Sci.* **60** 88–112
[47] Li X, Xiong Y, Qing G, Jiang G, Li X, Sun T and Liang X 2016 Bioinspired saccharide–saccharide interaction and smart polymer for specific enrichment of sialylated glycopeptides *ACS Appl. Mater. Interfaces* **8** 13294–302
[48] Qing G, Li X, Xiong P, Chen C, Zhan M, Liang X and Sun T 2016 Dipeptide-based carbohydrate receptors and polymers for glycopeptide enrichment and glycan discrimination *ACS Appl. Mater. Interfaces* **8** 22084–92
[49] Xiong Y, Li M, Lu Q, Qing G and Sun T 2017 Sialic acid-targeted biointerface materials and bio-applications *Polymers* **9** 249
[50] Dhand A P, Galarraga J H and Burdick J A 2021 Enhancing biopolymer hydrogel functionality through interpenetrating networks *Trends Biotechnol.* **39** 519–38
[51] Teixeira L S M, Feijen J, van Blitterswijk C A, Dijkstra P J and Karperien M 2012 Enzyme-catalyzed crosslinkable hydrogels: emerging strategies for tissue engineering *Biomaterials* **33** 1281–90
[52] Wu Q, Wang L, Ding P, Deng Y, Okoro O V, Shavandi A and Nie L 2022 Mercaptolated chitosan/methacrylate gelatin composite hydrogel for potential wound healing applications *Compos. Commun.* **35** 101344
[53] Jalili-Firoozinezhad S, Rajabi-Zeleti S, Mohammadi P, Gaudiello E, Bonakdar S, Solati-Hashjin M, Marsano A, Aghdami N, Scherberich A and Baharvand H 2015 Facile fabrication of egg white macroporous sponges for tissue regeneration *Adv. Healthcare Mater.* **4** 2281–90
[54] Zhang M, Lin P, Song X, Chen K, Yang Y, Xu Y, Zhang Q, Wu Y, Zhang Y and Cheng Y 2022 Injectable and self-healing hydrogels with tissue adhesiveness and antibacterial activity as wound dressings for infected wound healing *J. Polym. Sci.* **60** 1511–20
[55] Douglas T E L, Wlodarczyk M, Pamula E, Declercq H, de Mulder E L, Bucko M M, Balcaen L, Vanhaecke F, Cornelissen R and Dubruel P 2014 Enzymatic mineralization of gellan gum hydrogel for bone tissue-engineering applications and its enhancement by polydopamine *J. Tissue Eng. Regen. Med.* **8** 906–18
[56] Park K M, Lee Y, Son J Y, Bae J W and Park K D 2012 *In situ* SVVYGLR peptide conjugation into injectable gelatin-poly (ethylene glycol)-tyramine hydrogel via enzyme-mediated reaction for enhancement of endothelial cell activity and neo-vascularization *Bioconjugate Chem.* **23** 2042–50
[57] Jin R, Teixeira L M, Dijkstra P J, Van Blitterswijk C, Karperien M and Feijen J 2010 Enzymatically-crosslinked injectable hydrogels based on biomimetic dextran–hyaluronic acid conjugates for cartilage tissue engineering *Biomaterials* **31** 3103–13
[58] Lee F, Bae K H and Kurisawa M 2015 Injectable hydrogel systems crosslinked by horseradish peroxidase *Biomed. Mater.* **11** 014101
[59] Raia N R, Partlow B P, McGill M, Kimmerling E P, Ghezzi C E and Kaplan D L 2017 Enzymatically crosslinked silk-hyaluronic acid hydrogels *Biomaterials* **131** 58–67
[60] Sashiwa H, Makimura Y, Shigemasa Y and Roy R 2000 Chemical modification of chitosan: preparation of chitosan–sialic acid branched polysaccharide hybrids *Chem. Commun.* 11 909–10
[61] Vahdati M, Ducouret G, Creton C and Hourdet D 2020 Topology-specific injectable sticky hydrogels *Macromolecules* **53** 9779–92
[62] El Knidri H, Belaabed R, Addaou A, Laajeb A and Lahsini A 2018 Extraction, chemical modification and characterization of chitin and chitosan *Int. J. Biol. Macromol.* **120** 1181–9
[63] Nie L, Zou P, Feng S and Suo J 2013 Temperature-sensitive star-shaped block copolymers hydrogels for an injection application: phase transition behavior and biocompatibility *J. Mater. Sci. Mater. Med.* **24** 689–700
[64] Zou P, Suo J, Nie L and Feng S 2012 Temperature-sensitive biodegradable mixed star-shaped block copolymers hydrogels for an injection application *Polymer* **53** 1245–57
[65] Wang Z, Zhang Y, Yin Y, Liu J, Li P, Zhao Y, Bai D, Zhao H, Han X and Chen Q 2022 High-strength and injectable supramolecular hydrogel self-assembled by monomeric nucleoside for tooth-extraction wound healing *Adv. Mater.* **34** e2108300
[66] Dragan E S 2014 Design and applications of interpenetrating polymer network hydrogels. A review *Chem. Eng. J.* **243** 572–90
[67] Karoyo A H and Wilson L D 2021 A review on the design and hydration properties of natural polymer-based hydrogels *Materials* **14** 1095
[68] Sun W, Mu C, Zhang X, Shi H, Yan Q and Luan S 2022 Mussel-inspired polysaccharide-based sponges for hemostasis and bacteria infected wound healing *Carbohydrate Polym.* **295** 119868
[69] Liu S, Zhao Y, Wei H, Nie L, Ding P, Sun H, Guo Y, Chen T, Okoro O V and Shavandi A 2022 Injectable hydrogels based on silk fibroin peptide grafted hydroxypropyl chitosan and oxidized microcrystalline cellulose for scarless wound healing *Colloids Surf.* A **647** 129062